STUDY OF THE ORIENTATIONAL ORDERING OF CAROTENOIDS IN LIPID BILAYERS BY RESONANCE-RAMAN SPECTROSCOPY

M. VAN DE VEN, M. KATTENBERG, G. VAN GINKEL, AND Y. K. LEVINE
Biophysics Department, Physics Laboratory, University of Utrecht, 3584 CC Utrecht, The Netherlands

ABSTRACT The orientational ordering of β-carotene and crocetin embedded in lamellar model membranes has been investigated by angle-resolved resonance Raman scattering at a temperature well above the phase transition of the lipid chains. It is shown that the ordering of the carotenoids is dependent on the chemical composition of the lipid bilayers. The orientational distribution functions found clearly show that β-carotene is oriented parallel to the bilayer plane (dioleoyl lecithin) or perpendicular to it (soybean lecithin). For dimyristoyl lecithin at 40°C, egg-lecithin, and digalactosyl diacylglycerol two maxima were found in the orientational distribution: one parallel and one perpendicular to the bilayer surface. Crocetin embedded in soybean lecithin bilayers yields a similar bimodal distribution function. Because of rapid photodegradation no results could be obtained for spirilloxanthin.

INTRODUCTION

The carotenoids are known to act as accessory pigments in photosynthetic membranes and to protect chlorophyll from photooxidation (1). Although their functional properties have been intensively investigated, little is known about their organization in the membranes. To gain insight into their functional properties, their molecular behavior has been investigated in model membrane systems (2, 3). The orientation of carotenoids in lipid bilayers of different types has been studied by optical spectroscopy (2, 3), but with conflicting results. While some studies revealed that the molecules were preferentially oriented parallel to the plane of the bilayer (3), others indicated a preferential orientation in a perpendicular direction along the lipid chains (2).

Studies of molecular orientation using linear-dichroism techniques are known to yield information only about the second-rank order parameter $\langle P_2 \rangle$ of the absorbing species, $\langle P_2 \rangle = \langle 3\cos^2 \beta - 1 \rangle/2$, where β is the angle between the absorption transition moment and the local director, the normal to the bilayer surface. For carotenoids the absorption moment lies usually along the long molecular axis (5–9). However, a reliable reconstruction of the orientational statistics (11, 13, 14) requires knowledge of both $\langle P_2 \rangle$ and the fourth-rank order parameter $\langle P_4 \rangle$, $\langle P_4 \rangle = (35\langle \cos^4 \beta \rangle - 30\langle \cos^2 \beta \rangle + 3)/8$. Both these parameters can be determined from studies of angle-resolved depolarized Raman scattering. The Raman spectra of carotenoids can be resonance-enhanced by excitation within their absorption bands (4). The resonance-Raman spectra of carotenoids have been extensively studied (4–9) and are well understood.

We have used the resonance Raman effect to study the orientational statistics of carotenoid molecules incorporated into macroscopically ordered lipid bilayer systems. The order parameters, $\langle P_2 \rangle$ and $\langle P_4 \rangle$, of β-carotene and crocetin are reported. Other carotenoids were found to undergo severe photodegradation under our experimental conditions. The results indicate that the orientation of β-carotene and crocetin in the bilayer system strongly depends on the chemical composition of the lipids.

THEORY

The intensity of a Raman band I^μ associated with the normal coordinate μ of a molecular vibration and measured in a laboratory-fixed reference frame is proportional to (10)

$$I^\mu \sim \left\langle \left| \sum_{i,j} e_j^s \, \alpha_{\mu,ji} \, e_i^o \right|^2 \right\rangle, \tag{1}$$

where e_i^o and e_j^s are the cartesian components of the incident and scattered electric fields respectively. A second-rank real and symmetric polarizability tensor, $\underset{\sim}{\alpha}_\mu$, is associated with the molecular vibration and is assumed to include the local field effects arising from intermolecular interactions (11). The angled brackets denote an ensemble average over all the molecules in a macroscopic volume element.

The components of the tensor $\underset{\sim}{\alpha}_{\mathrm{MOL},\mu}$ in a molecule fixed frame are related to those in the laboratory frame by a rotational transformation

$$\underset{\sim}{\alpha}_{\mathrm{LAB},\mu} = \underset{\sim}{R}^{-1} \, \underset{\sim}{\alpha}_{\mathrm{MOL},\mu} \, \underset{\sim}{R}, \tag{2}$$

where all the information regarding the orientational distribution of the molecules relative to the macroscopic director is contained in the transformation matrix $\underset{\sim}{R}$. We shall find it convenient to carry out this transformation using Wigner rotation matrices $D^L_{mn}(\Omega)$ (12) and to express the tensor $\underset{\sim}{\alpha}$ in terms of its irreducible spherical components (12).

$$\alpha^{(0,0)} = -(\alpha_{xx} + \alpha_{yy} + \alpha_{zz})/3^{1/2}$$

$$\alpha^{(2,0)} = (2\alpha_{zz} + \alpha_{xx} - \alpha_{yy})/6^{1/2}$$

$$\alpha^{(2,\pm 1)} = \mp (\alpha_{xz} \pm i\,\alpha_{yz})$$

$$\alpha^{(2,\pm 2)} = (\alpha_{xx} - \alpha_{yy} \pm 2i\,\alpha_{xy})/2$$

so that we can rewrite Eq. 2 as

$$\alpha^{(2,m)}_{LAB,\mu} = \sum_n D^{2*}_{mn}(\Omega)\, \alpha^{(2,n)}_{MOL,\mu} \tag{3}$$

and $\alpha^{(0,0)}_{LAB,\mu} = \alpha^{(0,0)}_{MOL,\mu}$.

We shall also make use of the direct product $\underline{\underline{A}}$ of the unit vectors $\mathbf{e}^o$ and $\mathbf{e}^s$ describing, respectively, the polarization directions of the incident and scattered beams

$$\underline{\underline{A}} = \mathbf{e}^s \otimes \mathbf{e}^o . \tag{4}$$

The irreducible spherical components of $\underline{\underline{A}}$ are obtained according to reference 12. Thus Eq. 1 can be recast in the form

$$I^\mu \sim \left\langle \left| \sum_{L,m} A^{(L,m)} \alpha^{(L,m)*}_{LAB,\mu} \right|^2 \right\rangle$$

$$= \sum_{\substack{L,m,n \\ L',m',n'}} A^{(L,m)} A^{(L'm')*} \langle D^L_{mn} D^{L'*}_{m'n'} \rangle\, \alpha^{(L',n')}_{MOL,\mu}\, \alpha^{(L,n)*}_{MOL,\mu} \tag{5}$$

$$L,L' = 0, 1, 2; \quad m,n = -L, \ldots . L$$

$$m',n' = -L', \ldots . L'.$$

Eq. 5 can be simplified considerably by noting that the membrane samples possess a uniaxial symmetry about the macroscopic director (the normal to the plane of the sample) and a horizontal plane of symmetry. On using the Clebsch-Gordan series (12) we have

$$\langle D^L_{mn} D^{L'*}_{m'n'} \rangle = (-)^{m'-n'} \sum_{L''} C(LL'L''; m - m')\, C(LL'L''; n - n')\, \langle D^{L''}_{m-m',n-n'} \rangle . \tag{6}$$

The symmetry of the system requires $m = m'$ and $L'' = 0, 2, 4$. Further we shall assume the molecules to be cylindrically symmetric so that $n = n'$. Eq. 5 now reduces to

$$I^\mu \sim \sum_{L,L',m,n} A^{(L,m)} A^{(L',-m)} \langle D^L_{mn} D^{L'}_{-m-n} \rangle\, \alpha^{(L',-n)*}_{MOL,\mu}\, \alpha^{(L,n)*}_{MOL,\mu} \tag{7}$$

To enhance the Raman scattering intensities in our experiments, we make use of the resonance effect (10) and illuminate the molecules within their absorption band around 500 nm. Studies of carotene molecules in solutions (4–9) have shown that under these conditions the molecular polarizability tensor $\underline{\underline{\alpha}}$ is diagonal in the molecule-fixed frame and possesses only a single nonzero element, α_{zz}, for all the resonance-enhanced Raman modes. Here we take the z-axis of the molecular frame to lie along the long geometrical axis of the molecule. Consequently, we find $\alpha^{(0,0)}_{MOL} = -3^{-1/2}$ and $\alpha^{(2,m)}_{MOL} = (2/3)^{1/2}\delta_{m0}$, so that Eq. 7 becomes

$$I^\mu \sim \frac{1}{3}\{[A^{(0,0)}]^2 - 2\sqrt{2}\,\langle P_2 \rangle\, A^{(0,0)} A^{(2,0)} + 2\sum_{m=-2}^{2} G_m A^{(2,m)} A^{(2,-m)}\}, \tag{8}$$

where $G_m = \Sigma_{L=0,2,4}\, C(22L; m\ -m) C(22L; 00)\, \langle P_L \rangle$, where P_L is the Legendre polynomial of order L.

Consider the geometrical arrangement of the Raman experiment depicted in Fig. 1. This geometry is chosen so as to utilize the symmetry of the sample to ensure that only a single mode ray propagation takes place. Two polarization directions of the light can be used. The first, the ordinary ray (denoted as O, o) is polarized perpendicular to the plane of incidence and the second, the extraordinary ray (denoted as E, e), is polarized in that plane. The plane of incidence is the plane containing the beam of light and the normal, Z, to the surface of the sample (Fig. 1). We

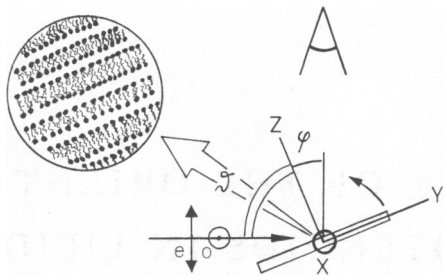

FIGURE 1 Experimental scattering geometry for a lamellar bilayer sample. XYZ is the director frame. θ and ϕ are the angles in air between the macroscopic director Z and the mutually perpendicular incident and scattered beams. e and o indicate the extraordinary and ordinary directions of polarization for the incident beam.

shall consider the exciting light to be incident at an angle θ relative to the macroscopic director and the scattered light will be observed at an angle ϕ. A perpendicular scattering geometry is used outside the sample. Here we shall neglect refraction effects, so that the angles used in the discussion refer to angles within the sample.

The unit vectors describing the directions of polarization of the beams are given by

$$\mathbf{e}^0_e \equiv (0, \cos\theta, \sin\theta); \quad \mathbf{e}^0_0 \equiv (1, 0, 0)$$

$$\mathbf{e}^s_e \equiv (0, -\cos\phi, \sin\phi); \mathbf{e}^s_0 \equiv (1, 0, 0).$$

We can carry out four independent intensity measurements: OO, OE, EE, EO, where the first letter denotes the polarization of the incident beam and the second that of the scattered beam. After some lengthy but straightforward algebra we obtain from Eq. 8 for the various intensities

$$I_{OO} \sim 3R_1 \tag{9a}$$

$$I_{OE} \sim (R_1 + R_2 \sin^2\phi) \tag{9b}$$

$$I_{EE} \sim [3R_1 + R_3 \sin^2\theta \sin^2\phi + R_4 \sin 2\theta \sin 2\phi + R_5(\sin^2\theta + \sin^2\phi)] \tag{9c}$$

$$I_{EO} \sim (R_1 + R_2 \sin^2\theta) \tag{9d}$$

where

$$R_1 = 1/15 - 2/21\,\langle P_2 \rangle + 1/35\,\langle P_4 \rangle$$

$$R_2 = 1/7\,(\langle P_2 \rangle - \langle P_4 \rangle)$$

$$R_3 = 4/15 + 4/21\,\langle P_2 \rangle + 19/35\,\langle P_4 \rangle$$

$$R_4 = 4/35\,\langle P_4 \rangle - 1/21\,\langle P_2 \rangle - 1/15$$

$$R_5 = 1/3\,\langle P_2 \rangle - 1/5\,\langle P_4 \rangle - 2/15 .$$

To eliminate the dependence of the measured intensities on unknown quantities, such as incident light intensity and illuminated volume, the depolarization ratios are defined as

$$R_o = I_{OE}/I_{OO} \qquad R_e = I_{EO}/I_{EE}, \tag{10}$$

where

$$R_o = \frac{1}{3} + \frac{R_2}{3R_1}\sin^2\phi \tag{11a}$$

$$R_e = \frac{R_1 + R_2 \sin^2\theta}{[3R_1 + R_3 \sin^2\theta \sin^2\phi + R_4 \sin 2\theta \sin 2\phi + R_5(\sin^2\theta + \sin^2\phi)]} . \tag{11b}$$

In deriving the theoretical relations above it was implicitly assumed that no refraction takes place at the air/glass and glass/membrane interfaces and that consequently no transmission losses occur. The appropriate Fresnel factors have been discussed in detail in reference (13) and used in the analysis of the experimental data. It can be shown further that the effects of multiple reflections within the sample will cause errors of <2% in the experimentally determined intensities, consequently, this effect will be negligible compared with the other experimental errors.

Eq. 11a shows that R_o is linearly dependent on $\sin^2\phi$, where ϕ is measured within the sample. The dependence of the slope $R_2/3R_1$, on $\langle P_4 \rangle$ for a number of $\langle P_2 \rangle$ values is shown in Fig. 2 *a*. We note here that the range of the physically allowed values of $\langle P_4 \rangle$ is determined by the inequalities (14) $1 \geq \langle P_4 \rangle \geq (35\langle P_2 \rangle^2 - 10\langle P_2 \rangle - 7)/18$ and $-3/7 \leq \langle P_4 \rangle \leq (5\langle P_2 \rangle + 7)/12$.

The angular dependence of R_e on the angle ϕ, measured in air, where $\theta + \phi = \pi/2$, for a number of $\langle P_2 \rangle$ and $\langle P_4 \rangle$ combinations is shown in Fig. 2 *b*. The calculated values were corrected for optical effects.

Both model calculations show that the polarization ratios, R_o and R_e, are insensitive to the orientational statistics in certain regions of the $\langle P_2 \rangle$, $\langle P_4 \rangle$ plane. Thus even small experimental errors will lead to relatively large inaccuracies in the derived values of the order parameters. The results presented here indicate that this is the case for all the systems studied.

The values of $\langle P_2 \rangle$ and $\langle P_4 \rangle$ were determined from the polarization ratios using Eq. 11. Eq. 11b for R_e can be linearized in terms of the two parameters. However, as this linear form proved to be sensitive to experimental errors, for the reasons given above, the results were checked by fitting the R_e data with Eq. 11b using nonlinear least squares methods.

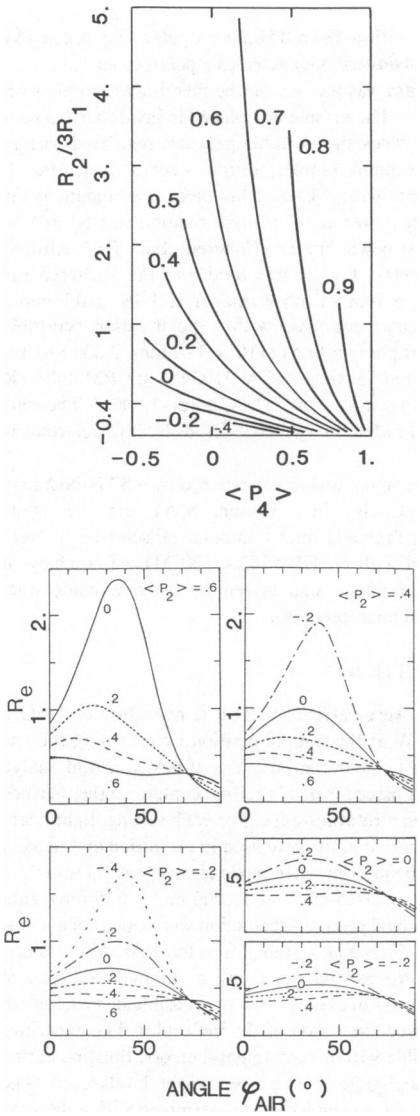

FIGURE 2 (*a*) The slope $R_2/3R_1$ of the ordinary depolarization ratio R_o (see text) vs. the fourth-rank orientational order parameter $\langle P_4 \rangle$. The values for the second-rank orientational order parameter $\langle P_2 \rangle$ are indicated. The refractive index n is 1.45. (*b*) The angular dependence of the extraordinary depolarization ratio R_e (see text) on the angle ϕ in air calculated for several combinations of $\langle P_2 \rangle$ and $\langle P_4 \rangle$. The refractive index n is 1.45.

EXPERIMENTAL

Materials

Egg lecithin was obtained from Lipid Products (South Nutfield, United Kingdom). Dimyristoyl-(DMPC), dioleoyl-phosphatidylcholine (DOPC) and all-*trans* β-carotene from carrots, type III, were purchased from Sigma Chemical Co. (St. Louis, MO). All-*trans* β-carotene was also prepared from *Anacystis nidulans* and spirilloxanthin (Fig. 3) was extracted from *Rhodospirillum rubrum* (17). Crocetin (Fig. 3) was purchased from Serva Feinbiochemica GmbH and Co. (Federal Republic of Germany), soybean lecithin and digalactosyl diacylglycerol (DGDG) were prepared from crude soybean lecithin (15) and spinach leaves, respectively (16), as described below. Ethanol and hexane were obtained from J.T. Baker Chemical Co. (Phillipsburg, NJ) (analytical reagent). Doubly distilled water was used.

Purification of Soybean Lecithin. Crude soybean lecithin was bought from V.N.R. Reformproducten B.V. Ede (The Netherlands) and prepurified by column chromatography on aluminium oxide 90 (Merck, Darmstadt, Federal Republic of Germany) using chloroform with increasing proportions of methanol as the eluent. The soybean lecithin fractions obtained were purified further by preparative high pressure liquid chromatography (HPLC) with the HPLC equipment described in reference 15 or with home-built HPLC equipment. As preparative chromatographic columns were used (*a*) 500 × 50 mm stainless steel (SS), packed with polygosil (60–1525; Machery Nagel and Co., Düren, Federal Republic of Germany); (*b*) 250 × 22.7 mm Lichrosorb Si-60-7 (SS) (Chrompack Nederland, Middelburg, The Netherlands). The columns were eluted with chloroform-methanol 70:30 (vol/vol). The fractions collected were analyzed for purity on silica gel 60 plates (10 × 10 cm, for nano-TLC, art 5633, Merck, Darmstadt, Germany). Chloroform/methanol/water [65:25:4 (vol/vol/vol)] was

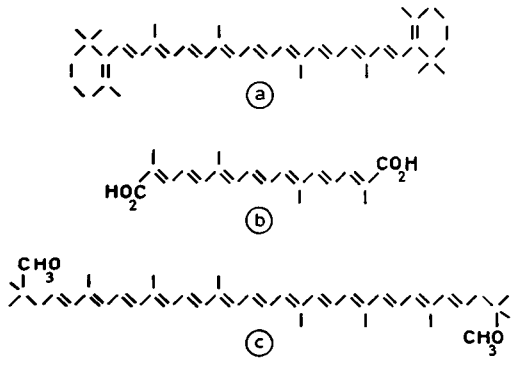

FIGURE 3 The molecular structure of (*a*) β-carotene, (*b*) crocetin, and (*c*) spirilloxanthin.

used as the eluting mixture. The fractions containing pure soybean lecithin were dried and stored dry under N_2 at $-20°C$.

Purification of DGDG from Spinach. Total lipid extraction from spinach chloroplasts and subsequent fractionation in lipid classes was performed as described in reference 16. The acetone fraction obtained, containing mainly galactolipids, was purified further by using preparative HPLC as described above. A Lichrosorb Si-60-7 column (SS, 250 × 22.7 mm; Chrompack Nederland) was used. The column was eluted with chloroform/methanol, 85:15(vol/vol). Analysis for purity was done as described above. We also used DGDG bought from Lipid Products. Analysis for purity was done as described. Only DGDG containing no contaminants by these criteria was used for our investigations.

Purification of Spirilloxanthin and of β-Carotene from Rhodospirillum Rubrum and from Anacystis Nidulans. The purification procedure for isolation of spirilloxanthin and β-carotene was based on the instructions described in reference 17. The crude pigment fractions obtained were purified further by thin layer chromatography (TLC) on precoated silica gel plates (Merck, Kieselgel 60, 0.25 mm) as described in reference 18. The bands containing either spirilloxanthin or β-carotene were scraped off and eluted with hexane. The pigments were analyzed for purity by (*a*) TLC, (*b*) absorption spectroscopy, and (*c*) Raman spectroscopy.

The lipids lecithin or DGDG in ethanol solution were mixed with solutions of β-carotene or crocetin. Stock solutions of 10^{-3} M β-carotene in hexane and crocetin in pyridine were freshly prepared. The final lipid-to-carotenoid molar ratio was 10^3:1. The samples were dried in the dark by flushing with nitrogen gas. Water was added gravimetrically to the dry material to form a 30% (wt/wt) mixture. The mixture was then allowed to equilibrate for 5 h at 37°C under a humidified nitrogen atmosphere.

Macroscopically oriented multibilayers were prepared by gently rubbing the hydrated lipid mixture between two microscope glass cover slips (thickness 175 ± 5 μm). This was done at room temperature except for DMPC, which was alined at 40°C. The alignment of the samples was monitored by optical microscopy following Asher and Pershan (26). Most samples of DMPC, DOPC, egg PC, and soybean PC contained oily streaks and appeared colored or inhomogeneous under the microscope in agreement with reference 26. However, ~10% of the samples exhibited excellent alignment over areas of ~1 cm^2. These areas were selected for further experimental work. In marked contrast, such problems were not encountered with DGDG, and well-aligned samples of this lipid were produced consistently. Well-oriented samples were sealed with a two component expoxy resin along their four rims. The thicknesses of the samples measured by dark field microscopy (26) were between 12 and 42 μm. For these measurements side illumination of the sample was used, so that light was reflected from the air/glass interfaces. The samples were viewed at their corners where small air pockets were present. The microscope, field depth 2 μm, was focused on the top surface of the sample and the objective was subsequently lowered with the vernier being turned in one direction only. The positions of the vernier on focusing the four interfaces were noted. This procedure was repeated several times at each corner of the sample. Furthermore measurements at the center revealed no curvature of the external coverslip surfaces across the samples.

Raman Setup

Angle resolved-polarized Raman spectra were obtained using the setup shown in Fig. 4. Spectra were obtained using an Ar^+-laser (model CR.18-UV; Coherent Inc., Palo Alto, CA) at 514.5 nm. An Anaspec-300S premonochromator was used to filter the plasma lines. To prevent sample heating, a Glan Taylor P10 laser polarizer (Halbo Optics, Guildford, Surrey, England) was used as an intensity regulator. A half wave plate (Jobin-Yvon; ISA Instruments, Longjumeau, Cedex, France) in conjunction with a Glan Thompson polarizing prism (Melles-Griot, Zevenaar, The Netherlands) acted as a polarization rotator.

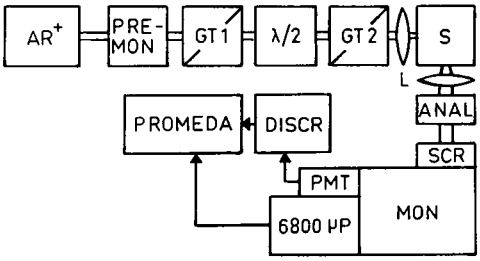

FIGURE 4 Raman setup. *Ar^+*, argon ion laser; *PREMON*, premonochromator; *GT1*, Glan Taylor polarizer; *λ/2*: half wave plate; *GT2*, Glan Thompson polarizer; *L*, lenses; *S*, sample; *ANAL*, analyzer; *SCR*, polarization scrambler; *MON*, double monochromator; *PMT*, photomultiplier tube; 6,800 μP, microcomputer; *DISCR*, discriminator; *PROMEDA*, microcomputer; for details see text.

The laser beam was focused on the membrane sample with a 101-mm focal length lens. The sample was placed in good thermal contact against a black copper block that was temperature regulated with a Colora K4 (Colora Messtechniek GmbH, Lorch, Federal Republic of Germany) thermostated circulating bath. This block was mounted on a rotating stage. The laser power at the sample position was 50 mW as measured with a CR 210 power meter (Coherent Inc., Palo Alto, CA). A 90° detection geometry, Fig. 1, was used and the scattered radiation was passed through a Jobin-Yvon Ramanor HG-2S double monochromator (ISA Instruments) equipped with a polarization scrambler and two concave, holographic gratings (110 × 110 mm, 2,000 grooves/mm) to a peltier-cooled, red sensitive RCA 31034 A-02 PM tube (RCA Corp., New York, NY) operating at −25°C and −1,800 V. The collection angle of the scattered radiation was 0.05 sterad. HN-32 polaroids were used as analyzers.

The PM tube signal was first processed by a STD-N-2 snap-off timing discriminator (Elscint Inc., Boston, MA) and then stored in, and displayed on, a Promeda microcomputer (Elscint Inc.). Net count rates were monitored with an HP 5383A 520 MHz frequency counter. The double monochromator was driven by a home-made microcomputer based on a 6800 microprocessor.

METHOD

Measurements were carried out at a temperature of 18°C with a laser power of 50 mW at the sample position by recording the angle resolved Raman spectra for four combinations of polarizer and analyzer settings. The sample was placed in good thermal contact on the thermostated block and mounted on a rotating stage. For each setting, light beams polarized vertically and horizontally were used in excitation and detection. Spectra were taken in the multiple scan mode (scan speed 200 cm^{-1}/min) at a slit width of 1,000 μm (6.5 cm^{-1} at 18,000 cm^{-1}, 556 nm). Integrated line intensities with background subtraction were calculated using a standard feature of the Promeda system after fourfold digital smoothing. The experiments were carried out using a random sequence of angles of incidence θ (Fig. 1) to average out any possible distortions arising from a systematic photodegradation of the molecules. The experimental results were reproducible within experimental errors, thus indicating that these effects were negligible at the laser power levels used. The refractive indices of membrane samples were determined with a thermostated Abbe refractometer (Bleeker Instruments, Utrecht, The Netherlands). Measurements at 514 nm were carried out with an expanded laser beam with greatly diminished intensity to prevent any damage to the eye.

RESULTS AND DISCUSSION

Resonance Raman spectra of the carotenoids in the lipid bilayers were measured well above the phase transition of

the chains at a temperature of 18°C for DGDG, DOPC, egg PC, and soybean PC and at 40°C for DMPC. A typical spectrum of β-carotene is shown in Fig. 5. The resonance enhanced peaks at 1,158 cm^{-1} and 1,525 cm^{-1} (accuracy 2 cm^{-1}) have been assigned (19–21) to the single-bond stretching mode ν_2 (═C—C═), and the double-bond stretching mode ν_1 (—C═C—), respectively. Laser power levels at the sample position were kept to 50 mW or less to avoid photoisomerisation processes. The formation of *cis*-isomers was easily detected by the appearance of a fairly strong line at ~1,250 cm^{-1} (22). The resonance Raman spectra of crocetin are similar to those of β-carotene, with the corresponding (—C═C—) peak at ~1,540 cm^{-1} (23). This is consistent with the shorter polyene chain length of the crocetin molecules.

Resonance Raman spectra of spirilloxanthin embedded in lipid bilayers could not be reproducibly obtained. This was due to the rapid photodegradation of the molecules. The depolarization ratios, R_e and R_o, for the resonance-enhanced modes above were measured in the membrane systems for 8–10 different values of the angle of incidence, measured in air. An accuracy of ~15% could be achieved. Typical angular dependences are shown in Fig. 6. A comparison with the model calculations shown in Fig. 2 indicates that the corresponding values of the order parameters are small and that further the results are expected to be sensitive to experimental errors. The depolarization ratios, R_o, measured in molecular solutions of β-carotene and crocetin, was found to be 0.333 ± 0.006 in agreement with the value found in reference 11, and R_e was 1.00 ± 0.01 as expected theoretically.

The refractive indices of the samples n_o and n_e for the ordinary and extraordinary rays, respectively, were measured as a function of temperature and the results for soybean PC are shown in Fig. 7. The small optical anisotropy observed can be neglected to a good approximation. The Fresnel corrections were calculated by considering the samples to be optically isotropic with a refractive index of 1.45.

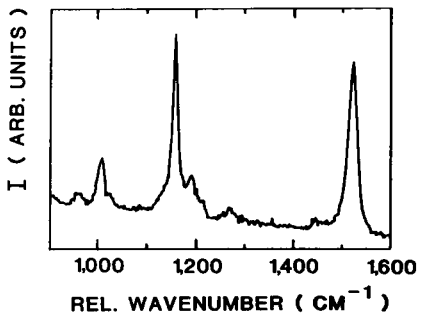

FIGURE 5 Resonance Raman spectrum of β-carotene in a lamellar lipid multibilayer system: soybean lecithin/water 70:30 (wt/wt) with 10^{-3} M β-carotene. Laser wavelength 514 nm. Laser power level at the sample position 50 mW. Sample temperature 18°C. (*Arb. units*), arbitrary units; *rel. wavenumber*, relative wavenumber.

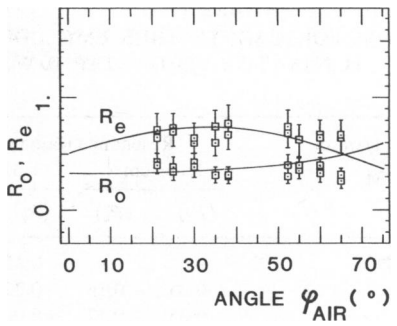

FIGURE 6 The angular dependence of the ordinary and extraordinary depolarization ratios R_o and R_e vs. the angle ϕ in air. Sample, egg lecithin/water 70:30 (wt/wt) with 10^{-3} M β-carotene. Laser wavelength 514 nm. Laser power at the sample position 50 mW. Lines, best fits for R_o and R_e.

Different samples of the same lipid species, which were judged to be well-aligned by optical microscopy, yielded reproducible values for the depolarization ratios, R_e and R_o, within experimental errors. In particular, a linear dependence of R_o on $\sin^2\phi$ (ϕ measured within the sample), was always observed in agreement with the theoretical prediction (Eq. 11a). This latter requirement was found to be a sensitive test of the quality of the samples. Thus samples exhibiting oily streaks or that appeared inhomogeneous and colored when viewed under the microscope yielded results at variance with Eq. 11a. Furthermore, the values of both the depolarization ratios, R_e and R_o, fluctuated strongly from sample to sample. These results indicate that the experiment monitors the orientation of carotene molecules embedded in the lipid bilayers and, moreover, that macroscopically the molecules are homogeneously distributed within the layers.

The values of the order parameters, $\langle P_2 \rangle$ and $\langle P_4 \rangle$, for the various samples are given in Table I. Their positions in the $\langle P_2 \rangle$, $\langle P_4 \rangle$ plane are also shown in Fig. 8, and the estimated absolute errors are indicated. The order parameters obtained from measurements of R_o and R_e were generally in excellent agreement. The value of $\langle P_2 \rangle$ in DOPC is further in good agreement with the value found in

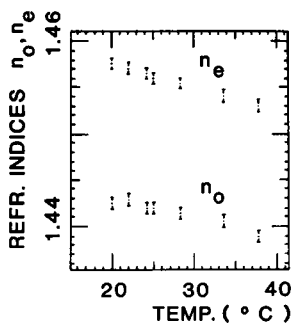

FIGURE 7 Ordinary and extraordinary refractive indices n_o and n_e vs. temperature T. Sample, soybean lecithin/water 70:30 (wt/wt) containing 10^{-3} M β-carotene. *Refr. indices*, refractive indices; *temp.*, temperature.

TABLE I

$\langle P_2 \rangle$ AND $\langle P_4 \rangle$ FOR CAROTENOIDS EMBEDDED IN VARIOUS (UN)SATURATED LIPID-WATER MIXTURES

70:30 (wt/wt) lipid/water mixture with 10^{-3}M β-carotene in:	Resonance Raman line 1,158 cm^{-1}		1,525 cm^{-1}	
	$\langle P_2 \rangle$	$\langle P_4 \rangle$	$\langle P_2 \rangle$	$\langle P_4 \rangle$
DMPC, T = 40°C	—	—	0.45	0.31
DOPC	−0.25	−0.13	−0.22	−0.13
Egg PC	−0.05	−0.17	−0.06	−0.16
Soybean PC	0.49	0.47	0.43	0.36
DGDG	0.12	0.10	0.05	0.05
10^{-3} M crocetin in:	1,530 cm^{-1}			
Soybean PC	0.19	0.36		

reference 3, which was determined from linear dichroism experiments. The results presented here clearly indicate that the orientation of the β-carotene molecules depends on the chemical composition of the lipid bilayers. This is in agreement with previous experiments in other systems (2, 3).

Fig. 8 shows that the observed values of $\langle P_2 \rangle$ and $\langle P_4 \rangle$ in all the systems studied here deviate significantly from those expected on the basis of a Gaussian orientational distribution, the so-called Maier-Saupe model (24). Thus, the determination of $\langle P_2 \rangle$ will only lead to erroneous conclusions about the orientational statistics of the carotene molecules in the lipid bilayers.

Note that the order parameters per se are simply averages of the Legendre polynomials P_2 and P_4 over the molecular distribution function $f(\beta)$. Consequently, their interpretation will depend on the assumed functional form of the distribution function. In a uniaxial membrane system $f(\beta)$ can be expressed (11) as a series expansion of Legendre polynomials $P_L(\cos\beta)$, each of which is weighted by an order parameter $\langle P_L \rangle$, which is the ensemble average of the corresponding term

$$f(\beta) = \tfrac{1}{2} \sum_{L=0} (2L + 1) < P_L > P_L(\cos\beta), \quad L \text{ even} \quad (12)$$

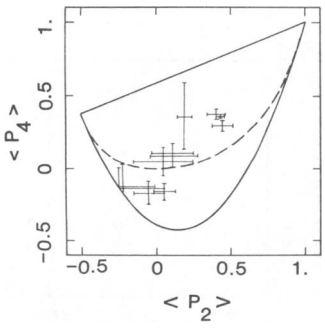

FIGURE 8 Plot of $\langle P_2 \rangle$ vs. $\langle P_4 \rangle$ as given in Table I for the various lipid bilayer systems. The continuous lines give the physical boundaries (see text) and the dashed line the results from a Gaussian orientational distribution function.

Thus $f(\beta)$ is fully characterized if all the $\langle P_L \rangle$'s are known. In practice, however, only $\langle P_2 \rangle$ and $\langle P_4 \rangle$ are accessible experimentally, so that the reconstruction of $f(\beta)$ using Eq. 12 must be truncated after the third term. There are two major objections to the use of such a truncated form of Eq. 12. First, such a truncation is physically equivalent to the assumption that all the order parameters $\langle P_L \rangle$ with $L \geq 6$ vanish identically. Clearly this assumption cannot be justified in general and that, consequently, the level of reliability of the resulting $f(\beta)$ cannot be judged. Second, $f(\beta)$ has the pathological property that it can become negative for a number of $\langle P_2 \rangle$ and $\langle P_4 \rangle$ combinations. We have therefore reconstructed the orientational distribution function $f(\beta)$ using an information-theoretic approach (25). Here the essential point is, that given the order parameters $\langle P_2 \rangle$ and $\langle P_4 \rangle$, the most probable values of $\langle P_L \rangle$, $L \geq 6$, are calculated under the assumption that the informational entropy of the system is a maximum (25). This corresponds to the construction of the broadest possible distribution function consistent with the known values of $\langle P_2 \rangle$ and $\langle P_4 \rangle$. It can then be shown that the resulting distribution function is of the form

$$f(\beta) = A \exp[\lambda_2 P_2(\cos\beta) + \lambda_4 P_4(\cos\beta)], \quad (13)$$

where A is a normalization constant, and λ_2 and λ_4 are determined using the known values of the order parameters, $\langle P_2 \rangle$ and $\langle P_4 \rangle$. We note here that Eq. 13 has the form of a Boltzmann distribution with an angle-dependent orienting potential. Representative distribution functions are shown in Fig. 9. We find that in DOPC bilayers the β-carotene molecules lie parallel to the bilayer surface with a high degree of alignment. In contrast the β-carotene molecules are oriented preferentially at right angles to the surface, and thus along the lipid chains, in bilayers of soybean PC. The distribution functions for β-carotene in bilayers of DMPC at 40°C, egg lecithin and DGDG, however, exhibit two maxima, one parallel and one perpendicular to the bilayer surface. This may, however, mean that we need to describe $f(\beta)$ in terms of two or more independent populations of β-carotene molecules.

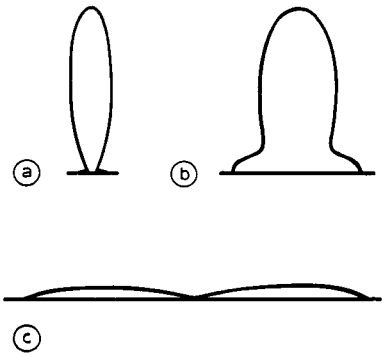

FIGURE 9 Orientational distribution functions $f(\beta)$ for (*a*) soybean lecithin, (*b*) DGDG, and (*c*) DOPC. The lipid-to-water ratio was 70:30 (wt/wt) for all samples.

The results obtained for crocetin embedded in bilayers of soybean PC also yield a bimodal distribution function with maxima parallel and perpendicular to the membrane surface. The foregoing analysis and the conclusions drawn about the orientation of the carotene molecules in the lipid bilayers are only tenable if the multibilayer samples satisfy two conditions. First, they must be free from oily streaks and other structural defects and second, the carotene molecules must not phase separate out of the lipids. At the beginning of this section we presented results indicating that the samples selected for the experiments meet both these conditions. Nevertheless, we point out that an alternative explanation of our findings might be that these conditions are not satisfied experimentally. If this is the case, our conclusions may not be relevant to the orientation of carotene molecules in lipid bilayers.

The authors are greatly indebted to Mrs. M.-L. Verheijden for careful preparation of the photosynthetic bacteria and to Dr. W. Verwer and Professor J. C. Goedheer for fruitful discussions.

Received for publication 21 June 1983 and in final form 27 December 1983.

REFERENCES

1. Goodwin, T. W. 1980. The biochemistry of carotenoids. *In* Plants. Chapman and Hall, New York. 1:77.
2. Yamamoto, H. Y., and A. D. Bangham. 1978. Carotenoid organization in membranes. Thermal transition and spectral properties of carotenoid-containing liposomes. *Biochim. Biophys. Acta.* 507:119–127.
3. Johansson, L. B.-Å., G. Lindblom, A. Wieslander, and G. Arvidson. 1981. Orientation of β-carotene and retinal in lipid bilayers. *FEBS (Fed. Eur. Biochem. Soc.) Lett.* 128:97–99.
4. Siebrand, W., and M. Z. Zgierski. 1979. Resonance Raman spectroscopy. A key to vibronic coupling. *In* Excited States. E. C. Lim, editor. Academic Press, Inc., New York. 4:1–136.
5. Warshel, A., and P. Dauber. 1977. Calculations of resonance Raman spectra of conjugated molecules. *J. Chem. Phys.* 66:5477–5488.
6. Lukashin, A. V., and M. D. Frank-Kamenetskii. 1978. Intensity distribution inside resonance Raman spectra of polyatomic molecules in solution. *Chem. Phys.* 35:469–476.
7. Siebrand, W., and M. Z. Zgierski. 1979. Frank-Condon effects in resonance Raman spectra and excitation profiles. *J. Chem. Phys.* 71:3561–3569.
8. Hoskins, L. C. 1981. Resonance Raman excitation profiles of lycopene. *J. Chem. Phys.* 74:882–885.
9. Ho, Z. Z., R. C. Hanson, and S. H. Lin. 1982. Experimental and theoretical studies of resonance Raman scatterings: Temperature effects in β-carotene. *J. Chem. Phys.* 77:3414–3423.
10. Koningstein, J. A. 1972. Introduction to the Theory of the Raman Effect. D. Reidel Publ. Comp., Dordrecht.
11. Pershan, P. S. 1979. Raman studies of orientational order in liquid crystals. *In* The Molecular Physics of Liquid Crystals. G. R. Luckhurst and G. W. Gray, editors. Academic Press, Inc., New York. 385–410.
12. Rose, M. E. 1957. Elementary Theory of Angular Momentum. J. Wiley and Sons, Inc., New York.
13. van der Meer, B. W., R. P. H. Kooyman, and Y. K. Levine. 1982. A theory of fluorescence depolarization in macroscopically ordered membrane systems. *Chem. Phys.* 66:39–50.
14. Kooyman, R. P. H., Y. K. Levine, and B. W. van der Meer. 1981. Measurement of second and fourth rank order parameters by fluorescence polarization experiments in a lipid membrane system. *Chem. Phys.* 60:317–326.
15. Geurts van Kessel, W. S. M., M. Tieman, and R. A. Demel. 1981. Purification of phospholipids by preparative high pressure lipid chromatography. *Lipids.* 16:58–63.
16. Fork, D. C., G. van Ginkel, and G. Harvey. 1981. Phase transition temperatures determined for chloroplast thylakoid membranes and for liposomes prepared from charged lipids extracted from thylakoid membranes of higher plants. *Plant Cell Physiol.* 22:1035–1042.
17. Liaaen-Jensen, S., and A. Jensen. 1971. Quantitative determination of carotenoids in photosynthetic tissues. *Methods Enzymol.* 23:586–602.
18. Swarthoff, T., H. J. M. Kramer, and J. Amesz. 1982. Thin-layer chromatography of pigments of the green photosynthetic bacterium Prosthecochloris aestuarii. *Biochim. Biophys. Acta.* 681:354–358.
19. Inagaki, F., M. Tasumi, and T. Miyazawa. 1974. Excitation profile of the resonance Raman effect of β-carotene. *J. Mol. Spectrosc.* 50:286–303.
20. Sufrà, S., G. Dellepiane, G. Masetti, and G. Zerbi. 1977. Resonance Raman spectrum of β-carotene. *J. Raman Spectrosc.* 6:267–272.
21. Verma, S. P., and D. F. H. Wallach. 1975. Carotenoids as Raman-active probes of erythrocyte membrane structure. *Biochim. Biophys. Acta.* 401:168–176.
22. Koyama, Y., M. Kito, T. Takii, K. Saiki, K. Tsukida, and J. Yamashita. 1982. Configuration of the carotenoid in the reaction centers of photosynthetic bacteria. Comparison of the resonance Raman spectrum of the reaction center of *Rhodopseudomonas sphaeroides* G1C with those of *cis-trans* isomers of β-carotene. *Biochim. Biophys. Acta.* 680:109–118.
23. Rimai, L., M. E. Heyde, and D. Gill. 1973. Vibrational spectra of some carotenoids and related linear polyenes. A Raman spectroscopic study. *J. Am. Chem. Soc.* 95:4493–4501.
24. Saupe, A., and W. Maier. 1961. Methoden zur Bestimmung des Ordnungsgrades nematischer Kristallinflüssiger Schichten. *Z. Naturforsch. A.* 16:816–824.
25. Berne, B.-J. 1971. Time dependent properties of condensed media. *In* Physical Chemistry. An Advanced Treatise. H. Eyring, D. Henderson, and W. Jost, editors. Academic Press, Inc., New York. 8:00.
26. Asher, S. A., and P. S. Pershan. 1979. Alignment and defect structures in oriented phosphatidylcholine multilayers. *Biophys. J.* 27:393–422.